

# Symmetry-dependent control of a spin qubit in lateral GaAs quantum dot

Pavle Stipsić<sup>1</sup> and Marko Milivojević<sup>2</sup>

<sup>1</sup>*Faculty of Physics, University of Belgrade, Studentski trg 12, 11001 Belgrade, Serbia*

<sup>2</sup>*NanoLab, QTP Center, Faculty of Physics, University of Belgrade, Studentski trg 12, 11001 Belgrade, Serbia*

We study the influence of quantum dot symmetry on the Rabi frequency and phonon induced spin relaxation rate in a single electron GaAs spin qubit. We find that anisotropic dependence on the magnetic field direction is independent of the choice of the gating potential. Also, we discover that relative orientation of the quantum dot, with respect to the crystallographic frame, is relevant in systems with  $C_{1v}$ ,  $C_{2v}$ , or  $C_n$  ( $n \neq 4r$ ) symmetry. To demonstrate the important impact of the gating potential shape on the spin qubit lifetime, we compare the effects of an equilateral triangle, square, and rectangular confinement with the known results for the harmonic potential. In the studied cases, enhanced spin qubit lifetime is revealed, reaching almost six orders of magnitude increase for the equilateral triangle gating.

PACS numbers: 81.07.Ta, 71.70.Ej, 72.10.Di, 76.30.v, 31.15.Hz

## I. INTRODUCTION

Every quantum two-level system can act as the quantum bit, a basic unit of quantum information processing [1, 2]. Among different solid-state implementations of the qubit system [3–6], single electron spin in a semiconductor quantum dot (QD) can be used to achieve the task. In order to manipulate spins of charge carriers embedded inside a semiconductor material electrically, through electric dipole spin resonance (EDSR) [7], the presence of spin-orbit interaction (SOI) is obligatory.

Beside its positive effect in EDSR based schemes [8–16], SOI enables the electron-phonon coupling mediated transitions between the qubit states [17–20], affecting the spin qubit lifetime. To suppress the coupling to phonons, different approaches like the optimisation of the QD design [21, 22] or control of the system size [23] were suggested. The observed anisotropy of the spin relaxation rate on the in-plane magnetic field orientation [24] offered another playground for fine-tuning of the spin qubit's desired properties. In circular QDs, this is the only degree of freedom accessible in the optimisation of the spin qubit, while for the elliptical confining potential [22, 25] orientation of the QD potential with respect to the crystallographic frame is accessible as the tuning parameter.

Evidently, different symmetry of the circular and elliptical potential is the main reason for the observed behaviour. But, to what extent can the potential symmetry alter the basic properties of the electrically controlled spin qubit? To address this question, we have performed a general analysis valid for the lateral GaAs QD system with  $C_{nv}$  or  $C_n$  symmetry of the gating potential. Besides the expected anisotropy on the magnetic field orientation, we were able to find potential symmetries for which the QD orientation with respect to the crystallographic frame can act as another control parameter of the spin qubit characteristics. With our theory we offer a simple and efficient way to determine the impact of the gating potential on the Rabi frequency and spin relaxation rate. This is shown on the example of anisotropic

and isotropic harmonic potential, as well as for equilateral triangle, square and rectangular potential.

This paper is organized as follows. In Section II we define a single electron GaAs spin qubit model. In Section III we define the dipole moment of the electrically controlled spin qubit that describes both the Rabi frequency and SOI induced spin relaxation rate mediated by acoustic phonons. In Section IV we present the main results of the paper, analytical expressions for the dipole moment in the case of the gating potential with  $C_{nv}$  or  $C_n$  symmetry. In Section V, to enlighten the impact of the gating potential on the spin qubit lifetime we use the obtained expressions to compare the influence of the harmonic confinement with equilateral triangle, square and rectangular potential. In Section VI we give our conclusions.

## II. DYNAMICS OF THE LATERAL QD

We start with the Hamiltonian describing the lateral dynamics of a single electron in the GaAs material

$$H = H_0 + H_z + H_{so} = \frac{p_x^2 + p_y^2}{2m^*} + V(x, y) + H_z + H_{so}, \quad (1)$$

where  $p_x$  and  $p_y$  are the momentum operators,  $m^*$  is the effective mass ( $m^* = 0.067m_e$  for GaAs,  $m_e$  is the electron mass), while  $V(x, y)$  is the gating potential used to localize the electron in a QD. In the lateral system, symmetries that can be present are the  $n$ -fold rotational symmetry and the vertical mirror plane symmetry  $\sigma_v$ . For simplicity, we will assume that  $\sigma_v$  coincides with the  $yz$ -plane of the QD coordinate frame (see FIG. 1). Thus, we assume a general form of the orbital Hamiltonian  $H_0$  that has a  $C_{nv}$  or  $C_n$  ( $n = \infty$  also) symmetry. Due to the symmetry, eigenenergies and eigenvectors of  $H_0$  can be classified according to the irreducible representations (IRs) of a given point group symmetry.

Besides  $H_0$ , in Eq. (1) the Zeeman term  $H_z$  appears,

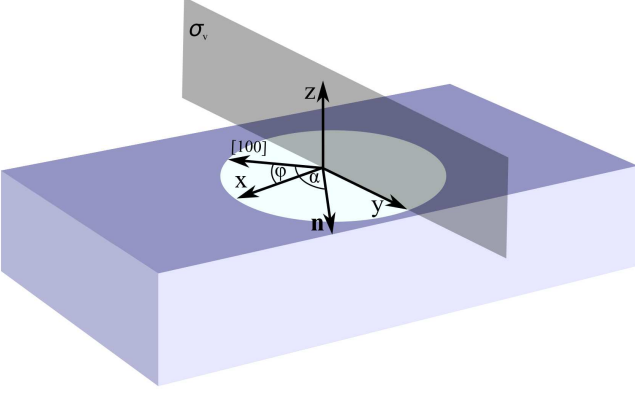


FIG. 1. A schematic view of the GaAs lateral QD. The  $y$ -axis of the QD reference frame coincides with the vertical mirror plane symmetry  $\sigma_v$ . We define the angle between the chosen  $x$ -axis and the crystallographic  $[100]$  axis as  $\varphi$ . Magnetic field is aligned along the  $\mathbf{n}$  direction, forming an angle  $\alpha$  with the  $[100]$  direction.

describing the coupling of spin and magnetic field

$$H_z = \frac{g}{2} \mu_B \mathbf{B} \cdot \boldsymbol{\sigma}, \quad (2)$$

where  $g$  is the effective Landé factor ( $g \approx -0.44$  for GaAs),  $\mu_B$  is the Bohr magneton, while  $\mathbf{B} = B\mathbf{n}$  is the in-plane magnetic field forming an angle  $\alpha$  with the crystallographic  $[100]$  axis. In Eq. (1) we have neglected the orbital effects of the magnetic field. This is a reasonable assumption for the magnetic field strength weaker than a few T [26].

Eigenstates of  $H_0 + H_z$  can be written in a direct product form  $|\Psi_i \pm\rangle = |\Psi_i\rangle \otimes |\pm\rangle$ , where  $|\Psi_i\rangle$  corresponds to the eigenvectors of the Hamiltonian  $H_0$  with an energy  $\epsilon_i$ , while  $|\pm\rangle$  represents eigenvectors of  $H_z$  with spin projection parallel/antiparallel to the magnetic field direction and an eigenenergy  $\pm g\mu_B B/2$ , respectively. The effect of  $H_z$  on the eigenspectra of  $H_0$  can be seen as the splitting of  $H_0$  eigenenergies into two branches with an energy difference  $|g|\mu_B B$ . In this work, we assume that  $|g|\mu_B B$  is much weaker than the energy difference between the ground and the first excited state of the orbital Hamiltonian  $H_0$ .

Beside  $H_0/H_z$  that acts trivially in the spin/orbital space, SOI Hamiltonian does not commute with  $H_0 + H_z$ . It consists of two terms, Dresselhaus [27] and Rashba [28]: Dresselhaus term exists due to the bulk inversion asymmetry of the structure, while the Rashba term is present when an electric field perpendicular to the growth direction is applied. The form of spin-orbit coupling is dependent on the structure's symmetry. For GaAs, having the zincblende structure, SOI Hamiltonian is equal to

$$H_{\text{so}} = \hbar \left( \frac{p_{[010]}\sigma_y - p_{[100]}\sigma_x}{2m^* l_d} + \frac{p_{[100]}\sigma_y - p_{[010]}\sigma_x}{2m^* l_r} \right), \quad (3)$$

where  $l_r = 2.42\mu\text{m}$  and  $l_d = 0.63\mu\text{m}$  [26, 29] are Rashba and Dresselhaus confinement lengths, respectively, while

$l = 10\text{nm}$  [26, 29] represents typical confinement length of the GaAs QD in an experimental setup. Note that, in Eq. (3), operators  $p_{[100]}$  and  $p_{[010]}$  are the momentum operators written in the crystallographic frame. We have the choice to define the  $x$ -axis of our coordinate frame independently on the crystallographic  $[100]$  direction. Assuming that the angle between them is  $\varphi$ ,  $p_{[100]}$  and  $p_{[010]}$  should be written in terms of momentum operators in the chosen frame:  $p_{[100]} = p_x \cos \varphi - p_y \sin \varphi$ ,  $p_{[010]} = p_x \sin \varphi + p_y \cos \varphi$ .

To compare the ratio of the spin-orbit length and  $l$ , we redefine  $l_r$  and  $l_d$  in terms of the overall spin-orbit length  $l_{\text{so}}$  and the spin-orbit angle  $\nu$

$$l_d^{-1} = l_{\text{so}}^{-1} \sin \nu, \quad l_r^{-1} = l_{\text{so}}^{-1} \cos \nu. \quad (4)$$

Since  $l_{\text{so}} \gg l$ , SOI can be treated as a perturbation.

Without SOI, qubit states can be defined as  $|\Psi_0 \pm\rangle = |\Psi_0\rangle \otimes |\pm\rangle$ , where  $|\Psi_0\rangle$  corresponds to the ground state of the spin-independent Hamiltonian  $H_0$ . Since SOI can be treated on the level of a perturbation, we calculate first-order corrections of the qubit states due to spin-orbit coupling. Following the procedure explained in [22], we first transform the Hamiltonian  $H$  using the unitary operator  $U = \exp(i\mathbf{n}_{\text{so}} \cdot \boldsymbol{\sigma}/2)$ , defined with the help of the position dependent spin-orbit vector  $\mathbf{n}_{\text{so}} = l_{\text{so}}^{-1}(r_{[100]} \sin \nu + r_{[010]} \cos \nu, -r_{[100]} \cos \nu - r_{[010]} \sin \nu, 0)$ ,

$$U H U^\dagger = H_0 + H_z + H_{\text{so}}^{\text{eff}}. \quad (5)$$

The unitary operator  $U$  does not change the orbital and Zeeman Hamiltonian. On the other hand, the SOI Hamiltonian  $H_{\text{so}}$  is transformed into

$$H_{\text{so}}^{\text{eff}} = \frac{g\mu_B}{2} (\mathbf{n}_{\text{so}} \times \mathbf{B}) \cdot \boldsymbol{\sigma} - \frac{\hbar^2}{4m^* l_{\text{so}}^2} \left( 1 + l_z \sigma_z \cos 2\nu \right), \quad (6)$$

where  $l_z = -i(r_{[100]} \partial_{r_{[010]}} - r_{[010]} \partial_{r_{[100]}})$  is the orbital angular momentum. Using the  $H_{\text{so}}^{\text{eff}}$ , first-order correction of the qubit states can be written as

$$\delta|\Psi_0 \sigma\rangle = U \sum_{i \neq 0, \beta} \frac{\langle \Psi_i \beta | H_{\text{so}}^{\text{eff}} | \Psi_0 \sigma \rangle}{\epsilon_0 - \epsilon_i + \frac{\sigma - \beta}{2} g\mu_B B} |\Psi_i \beta\rangle, \quad (7)$$

where the sum over  $i \neq 0$  correspond to all orbital eigenvectors  $|\Psi_i\rangle$  different from the ground state  $|\Psi_0\rangle$ , while  $\beta = \pm$ .

Lateral QD model is valid if the electron dynamics in the  $z$ -direction is suppressed, i.e. an electron is always in the ground state. Thus, we assume that confinement length in the  $z$ -direction is much stronger than in the  $xy$ -plane. Hamiltonian describing the quantum confinement in the  $z$ -direction is equal to  $H(z) = p_z^2/2m^* + V(z)$ , where  $V(z) = eE_0 z$  for  $z \geq 0$  and  $V(z) = \infty$  for  $z < 0$ . To this Hamiltonian corresponds the following ground state (for  $z > 0$ ) [30]

$$\Psi_0(z) = 1.4261\sqrt{\chi} \text{Ai}(\chi z - 2.3381), \quad (8)$$

where  $\text{Ai}$  is the Airy function, while  $\chi = (2m^*eE_0/\hbar^2)^{1/3}$  is the inverse of the characteristic length  $z_0 = 1.5587/\chi$  in the  $z$ -direction.

In order to simplify the notation, in the rest of the paper we will assume that  $|\uparrow\rangle$  and  $|\downarrow\rangle$  represent SOI corrected qubit states in the  $xy$ -plane, while  $|\Psi_\uparrow\rangle = |\uparrow\rangle\Psi_0(z)$  and  $|\Psi_\downarrow\rangle = |\downarrow\rangle\Psi_0(z)$  correspond to wavefunctions of the qubit states in three dimensions.

### III. RABI FREQUENCY AND PHONON INDUCED SPIN RELAXATION RATE

Electrical control of the spin qubit is possible by applying the in-plane oscillating electric field  $\mathbf{E}\cos\omega t$ , resulting in the Rabi Hamiltonian  $H_R = e\mathbf{E} \cdot \mathbf{r}\cos(\omega t)$ . Rabi frequency, measuring the speed of the single-qubit rotations, is equal to  $\Omega = e/\hbar|\mathbf{E} \cdot \langle\uparrow|\mathbf{r}|\downarrow\rangle|$ , where

$$\mathbf{d}_{\uparrow\downarrow} = \langle\uparrow|\mathbf{r}|\downarrow\rangle \quad (9)$$

is the dipole moment (in  $e$  units), present due to the SOI induced spin mixing mechanism. Misalignment of the applied field direction and the dipole moment leads to a trivial suppression of the Rabi frequency. Since it is beneficial to increase the Rabi frequency as much as possible, the electric field should be applied in the direction of the dipole moment. Thus, for fixed  $|\mathbf{E}|$ , the maximal value  $\max(\Omega) = \Omega_{\uparrow\downarrow}$  of Rabi frequency

$$\Omega_{\uparrow\downarrow} = \frac{e}{\hbar}|\mathbf{E}||\mathbf{d}_{\uparrow\downarrow}| \quad (10)$$

is completely dependent on the strength of the dipole moment.

Besides enabling the electrical control of a spin qubit, SOI triggers the undesired phonon induced transition between the qubit states, setting up a limit on the qubit lifetime. The rate of spin relaxation at  $T = 0$  can be determined from the Fermi golden rule

$$\Gamma_{\uparrow\downarrow} = \frac{2\pi}{\hbar} \sum_{\nu\mathbf{q}} |M_\nu(\mathbf{q})|^2 |\langle\Psi_\uparrow|e^{i\mathbf{q}\cdot\mathbf{r}_c}|\Psi_\downarrow\rangle|^2 \delta(\epsilon_{\uparrow\downarrow} - \hbar\omega_{\nu\mathbf{q}}). \quad (11)$$

Spin relaxation is induced by acoustic phonons of an energy  $\hbar\omega_{\nu\mathbf{q}}$ , equal to the level separation between the qubit states,  $\epsilon_{\uparrow\downarrow} = |g|\mu_B B$ . For magnetic field strengths up to a few T, relevant for this work, linear dependence of phonon frequencies on the crystal wave vector intensity can be used,  $\omega_{\nu\mathbf{q}} = c_\nu|\mathbf{q}|$ , giving us  $|\mathbf{q}| = |g|\mu_B B/\hbar c_\nu$  [31].

Geometric factor  $|M_\nu(\mathbf{q})|^2$  is dependent on phonon mode, longitudinal (LA) or transverse (TA). The longitudinal geometric factor [32]

$$|M_{\text{LA}}(\mathbf{q})|^2 = \frac{\hbar D^2}{2\rho c_{\text{LA}} V} |\mathbf{q}| + \frac{32\pi^2 \hbar (eh_{14})^2}{\epsilon^2 \rho c_{\text{LA}} V} \frac{(3q_x q_y q_z)^2}{|\mathbf{q}|^7} \quad (12)$$

depends on both  $D$  and  $h_{14}$ , representing the deformation and piezoelectric constant, respectively. On the other hand, the transverse geometric factor [32]

$$|M_{\text{TA}}(\mathbf{q})|^2 = 2 \frac{32\pi^2 \hbar (eh_{14})^2}{\epsilon^2 \rho c_{\text{TA}} V} \times \left| \frac{q_x^2 q_y^2 + q_x^2 q_z^2 + q_y^2 q_z^2}{|\mathbf{q}|^5} - \frac{(3q_x q_y q_z)^2}{|\mathbf{q}|^7} \right|, \quad (13)$$

is dependent on the piezoelectric constant solely. Other parameters for the GaAs material are [22, 33]:  $c_{\text{LA}} = 5290\text{m/s}$ ,  $c_{\text{TA}} = 2480\text{m/s}$ ,  $\rho = 5300\text{kg/m}^3$ ,  $D = 7\text{eV}$ ,  $eh_{14} = 1.4 \times 10^9\text{eV/m}$ , and  $\epsilon = 12.9$ .

Finally, in Eq. (11) both the lateral and the  $z$ -direction confinement enter the relaxation rate through the scattering matrix element  $|\langle\Psi_\uparrow|e^{i\mathbf{q}\cdot\mathbf{r}_c}|\Psi_\downarrow\rangle|^2$ . We employ the dipole approximation  $e^{i\mathbf{q}\cdot\mathbf{r}_c} \approx 1 + i\mathbf{q} \cdot \mathbf{r}_c$ , justified for magnetic field strengths below few T.

To summarize, phonon induced relaxation rate can be divided in three separate channels: of the deformation phonons  $\Gamma_{\uparrow\downarrow}^{\text{def}}$ , of the longitudinal piezoelectric phonons  $\Gamma_{\uparrow\downarrow}^{\text{piez,LA}}$ , and of the transverse piezoelectric phonons  $\Gamma_{\uparrow\downarrow}^{\text{piez,TA}}$ . In GaAs QDs,  $\Gamma_{\uparrow\downarrow}^{\text{piez,TA}}$  is the dominant relaxation channel, being two orders of magnitude stronger than  $\Gamma_{\uparrow\downarrow}^{\text{piez,LA}} + \Gamma_{\uparrow\downarrow}^{\text{def}}$  in the dipole approximation regime. Thus, we can identify the total relaxation rate with  $\Gamma_{\uparrow\downarrow}^{\text{piez,TA}}$  [34]

$$\Gamma_{\uparrow\downarrow} = \frac{256\pi (eh_{14})^2 (|g|\mu_B B)^3}{105c_{\text{TA}}^5 \rho \hbar^4 \epsilon^2} \left(1 + \frac{7}{33} K_{\text{TA}}^2 z_0^2\right) |\mathbf{d}_{\uparrow\downarrow}|^2, \quad (14)$$

where  $K_{\text{TA}} = |g|\mu_B B/\hbar c_{\text{TA}}$ .

Note that  $\Gamma_{\uparrow\downarrow}$  is square dependent on the intensity of the dipole moment, meaning that the knowledge of the dipole moment is sufficient to fully explain the behaviour of both the Rabi frequency and spin relaxation rate.

### IV. ANALYTICAL EXPRESSION FOR THE DIPOLE MOMENT

Based on the previous conclusion, we come to the main objective: to derive symmetry allowed expression for the dipole moment. The results can be divided in three cases, according to the system's group symmetry: (A)  $\mathbf{C}_{nv}$  ( $n \geq 3$ ) and  $\mathbf{C}_{\infty v}$ , (B)  $\mathbf{C}_{2v}$  and  $\mathbf{C}_{1v}$ , or (C)  $\mathbf{C}_n$  and  $\mathbf{C}_\infty$ .

#### A. Dipole moment for systems with $\mathbf{C}_{nv}$ ( $n \geq 3$ ) or $\mathbf{C}_{\infty v}$ symmetry

To find the SOI induced perturbative correction of the qubit states, we first rewrite the unitarily transformed SOI Hamiltonian in the coordinate frame of the potential

$$H_{\text{so}}^{\text{eff}} = \frac{g\mu_B B}{2} \sigma_z \left( x(\sin(\nu + \varphi) \sin \alpha + \cos(\nu - \varphi) \cos \alpha) + y(\cos(\nu + \varphi) \sin \alpha + \sin(\nu - \varphi) \cos \alpha) \right) \quad (15)$$

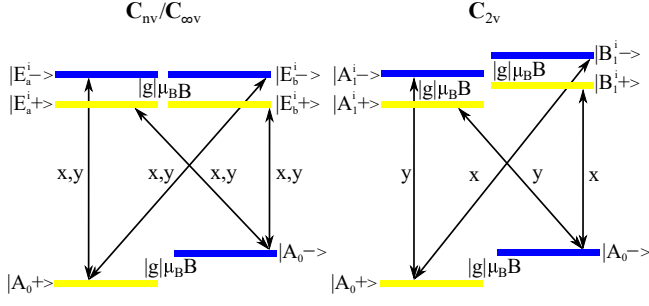


FIG. 2. A schematic view of the first-order perturbation correction of the qubit states  $|A_0\pm\rangle$  in the case of  $\mathbf{C}_{nv}(\mathbf{C}_{\infty v})$  (left panel) and  $\mathbf{C}_{2v}$  (right panel) symmetry. In the first case, states that correct the qubit states have the two-fold orbital degeneracy and transform according to the IR  $E_1$ . These states are split by the Zeeman energy  $|g|\mu_B B$ . Transition between the SOI uncorrected qubit states and the  $|E_{a,b}^i\rangle$  states is enabled by the  $x$  and  $y$  terms from  $H_{so}^{\text{eff}}$ . In the second case, orbital states involved in the qubit states correction transform according to IRs  $A_1$  and  $B_1$ ; transition is triggered by the terms  $y$  and  $x$  from  $H_{so}^{\text{eff}}$ , respectively.

and neglect the second term in Eq. (6), assuming magnetic field strengths  $> \mu T$ , needed to appropriately define the qubit states. For simplicity, we define two factors

$$v_x = \sin(\nu + \varphi) \sin \alpha + \cos(\nu - \varphi) \cos \alpha, \quad (16)$$

$$v_y = \cos(\nu + \varphi) \sin \alpha + \sin(\nu - \varphi) \cos \alpha, \quad (17)$$

with whose help  $H_{so}^{\text{eff}}$  can be written in a more compact form.

Hamiltonian  $H_{so}^{\text{eff}}$  is in the orbital space dependent on the coordinates  $x$  and  $y$  that transform according to the IR  $E_1$ . Their symmetry behaviour restricts the states that can appear in the perturbative correction of the qubit states. It is simple to check that only states transforming according to the IR  $E_1$  are allowed. This is illustrated on the left panel of FIG. 2.

We label the ground state of the orbital Hamiltonian as  $|A_0\rangle$ , since the ground state in quantum mechanical systems is of the maximal possible symmetry [35] and it should transform according to the  $A_0$  IR, representing the objects invariant under all group symmetry operations (see Table I). We write two complex conjugate basis vectors of the two-dimensional IR  $E_1$  as  $|E_a^i\rangle$  and  $|E_b^i\rangle$ , where  $i$  labels the energy level. Also, we define the energy difference between the excited level and the ground state as  $\epsilon^i = \epsilon_{ex}^i - \epsilon_{gr}$ .

Due to the negative  $g$  factor, the lowest qubit state  $|A_0+\rangle = |A_0\rangle \otimes |+\rangle$  is parallel to the magnetic field direction, while  $|A_0-\rangle = |A_0\rangle \otimes |-\rangle$  is the qubit state with spin projection antiparallel to the magnetic field direction. First-order perturbative correction to the qubit states shall be written as  $|\delta A_0\pm\rangle$ . Thus, we can write the SOI corrected qubit states as  $|\uparrow\downarrow\rangle = |A_0\pm\rangle + |\delta A_0\pm\rangle$ , where the normalization factor is omitted as the correc-

TABLE I. For  $\mathbf{C}_{nv}$  and  $\mathbf{C}_{\infty v}$  symmetry groups, tables of matrices of the corresponding IRs are given [36], tabulated on the generators  $C_n(R_\beta)$  and  $\sigma_v$ , where  $C_n(R_\beta)$  represents a rotation for the angle  $2\pi/n(\beta)$  around the  $z$ -axis. In the  $\mathbf{C}_{nv}$  case, two-dimensional IRs exist if  $n \geq 3$ . In both cases, two-dimensional IRs are written in a complex conjugate basis.

$\mathbf{C}_{nv}$	IR	$m$	$C_n$	$\sigma_v$
	$A_0/B_0$	0	1	$\pm 1$
	$E_m$	$(0, \frac{n}{2})$	$\begin{pmatrix} e^{i\frac{2\pi}{n}m} & 0 \\ 0 & e^{-i\frac{2\pi}{n}m} \end{pmatrix}$	$\begin{pmatrix} 0 & 1 \\ 1 & 0 \end{pmatrix}$
	$A_{\frac{n}{2}}/B_{\frac{n}{2}}$	$\frac{n}{2}$	-1	$\pm 1$
$\mathbf{C}_{\infty v}$	IR	$m$	$R_\beta$	$\sigma_v$
	$A_0/B_0$	0	1	$\pm 1$
	$E_m$	1, 2, ...	$\begin{pmatrix} e^{i\beta m} & 0 \\ 0 & e^{-i\beta m} \end{pmatrix}$	$\begin{pmatrix} 0 & 1 \\ 1 & 0 \end{pmatrix}$

tion is small. Thus, the dipole moment is equal to

$$\mathbf{d} = \sum_{j=x,y} \langle \uparrow | \mathbf{r} \cdot \mathbf{e}_j | \downarrow \rangle \mathbf{e}_j = \sum_{j=x,y} \left( \langle A_0+ | \mathbf{r} \cdot \mathbf{e}_j | \delta A_0- \rangle \mathbf{e}_j + \langle \delta A_0+ | \mathbf{r} \cdot \mathbf{e}_j | A_0- \rangle \mathbf{e}_j \right). \quad (18)$$

Since  $l_{so} \gg l$ , we approximate the unitary operator  $U$  with  $I_2$ , where  $I_2$  is the identity  $2 \times 2$  matrix. After noticing that  $\langle \pm | \sigma_z | \mp \rangle = -1$ ,  $\langle \pm | \sigma_z | \pm \rangle = 0$ , we find the SOI induced corrections of the qubit states

$$|\delta A_0\pm\rangle = \frac{|g|\mu_B B}{2l_{so}} \sum_i \left( \frac{\langle E_a^i | x v_x + y v_y | A_0 \rangle}{\epsilon^i \pm |g|\mu_B B} |E_a^i \mp\rangle + \frac{\langle E_b^i | x v_x + y v_y | A_0 \rangle}{\epsilon^i \pm |g|\mu_B B} |E_b^i \mp\rangle \right). \quad (19)$$

Additionally, transition dipole matrix elements are labeled as

$$X^i = \langle E_a^i | x | A_0 \rangle, \quad Y^i = \langle E_a^i | y | A_0 \rangle. \quad (20)$$

Since the Zeeman splitting is much smaller than the orbital excitation energies,  $|g|\mu_B B \ll \epsilon^i$ , approximation  $\epsilon^i \pm |g|\mu_B B \approx \epsilon^i$  can be made. Thus, Eq. (19) is transformed into

$$|\delta A_0\pm\rangle = \frac{|g|\mu_B B}{2l_{so}} \sum_i \left( \frac{X^i v_x + Y^i v_y}{\epsilon^i} |E_a^i \mp\rangle + \frac{(X^i)^* v_x + (Y^i)^* v_y}{\epsilon^i} |E_b^i \mp\rangle \right), \quad (21)$$

where  $(X^i)^*$  and  $(Y^i)^*$  are the complex conjugates of  $X^i$  and  $Y^i$ , respectively. Components of the dipole moment



can now be written in a more compact form

$$\begin{aligned} d_x &= \frac{|g|\mu_B B}{l_{\text{so}}} \sum_i \left( \frac{2|X^i|^2 v_x + (X^i(Y^i)^* + (X^i)^* Y^i) v_y}{\epsilon^i} \right), \\ d_y &= \frac{|g|\mu_B B}{l_{\text{so}}} \sum_i \left( \frac{2|Y^i|^2 v_y + (X^i(Y^i)^* + (X^i)^* Y^i) v_x}{\epsilon^i} \right). \end{aligned} \quad (22)$$

Potential dependent parameters that enter the Eq. (22) are the transition dipole matrix elements and the excitation energies. Beside them, dipole moment components are dependent on the spin-orbit angle  $\nu$ , magnetic field angle  $\alpha$ , and the angle  $\varphi$  between the [100] crystallographic direction and the  $x$ -axis.

A further simplification of the Eq. (22) stems from the existence of the vertical mirror symmetry  $\sigma_v$ , requiring that  $X^i(Y^i)^* + (X^i)^* Y^i$  must be zero. This can be proven in a few simple steps. First, we deduce from the matrix of an IR  $E_1$ , representing the vertical mirror plane, that  $\sigma_v$  transforms one IR vector into the other,  $E_1(\sigma_v)|E_{a,b}^i\rangle = |E_{b,a}^i\rangle$ . Furthermore,  $y$  remains unchanged, while  $x$  acquires a minus sign, leading to the following behaviour of the transition matrix elements  $X^i$  and  $Y^i$  under vertical mirror plane symmetry

$$X^i \xrightarrow{\sigma_v} -(X^i)^*, Y^i \xrightarrow{\sigma_v} (Y^i)^*. \quad (23)$$

From the previous relations, we conclude that the term  $X^i(Y^i)^* + (X^i)^* Y^i$  transforms into  $-(X^i(Y^i)^* + (X^i)^* Y^i)$ , meaning that this object does not obey the symmetry of a system and must vanish.

Additionally, rotational symmetry of a system imposes that matrix elements  $|X^i|^2$  and  $|Y^i|^2$  are equal. This can be concluded from the action of the rotation  $C_n$  for an angle  $\beta_n = 2\pi/n$  around the  $z$ -axis, being the element of the group symmetry. An element  $C_n$  leaves the vector  $|A_0\rangle$  unchanged and adds a phase  $\exp(i\beta_n)$  to the vector  $|E_a^i\rangle$ . Also, it transforms  $x$  and  $y$  to  $x \cos \beta_n + y \sin \beta_n$  and  $-x \sin \beta_n + y \cos \beta_n$ . Thus,  $X^i$  and  $Y^i$  are transformed into  $\exp(-i\beta_n)(X^i \cos \beta_n + Y^i \sin \beta_n)$  and  $\exp(-i\beta_n)(-X^i \sin \beta_n + Y^i \cos \beta_n)$ , respectively. Correspondingly,

$$\begin{aligned} |X^i|^2 &\xrightarrow{C_n} |X^i|^2 \cos^2 \beta_n + |Y^i|^2 \sin^2 \beta_n, \\ |Y^i|^2 &\xrightarrow{C_n} |X^i|^2 \sin^2 \beta_n + |Y^i|^2 \cos^2 \beta_n, \end{aligned} \quad (24)$$

where we have neglected the  $X^i(Y^i)^* + (X^i)^* Y^i$  term, being previously proven to equal to zero. Since  $|X^i|^2$  and  $|Y^i|^2$  must remain unchanged under the group symmetry operations, we conclude that relation  $|X^i|^2 = |Y^i|^2$  must hold. Thus, we have obtained a general relation for the dipole moment in the case of the potential symmetry  $\mathbf{C}_{nv}$  ( $n \geq 3$ )

$$\mathbf{d}_{\uparrow\downarrow}^{\mathbf{C}_{nv}} = \frac{2|g|\mu_B B}{l_{\text{so}}} \left( \sum_i \frac{|X^i|^2}{\epsilon^i} \right) (v_x \mathbf{e}_x + v_y \mathbf{e}_y). \quad (25)$$

In these situations, intensity of the dipole moment  $|\mathbf{d}_{\uparrow\downarrow}^{\mathbf{C}_{nv}}|^2 \sim (1 + \sin 2\alpha \sin 2\nu)$  is independent on the orientation of the potential with respect to the crystallographic frame.

Analogous analysis can be conducted in the  $\mathbf{C}_{\infty v}$  case. Since the matrix form of the IRs  $A_0$  and  $E_1$  (see Table I) for this symmetry group is the same as for  $\mathbf{C}_{nv}$ , the procedure is exactly the same if the change  $\beta_n \rightarrow \beta$  in the previous discussion is made.

As an example, we implement the derived formula (25) in the case of the isotropic two-dimensional harmonic confinement  $V^{\text{iho}}(x, y) = 1/2m^*\omega^2(x^2 + y^2)$  with  $\mathbf{C}_{\infty v}$  symmetry, assuming only one excited level in the perturbative correction of the qubit states. With the help of the states  $\psi_0$  and  $\psi_1$ , corresponding to the ground and the first excited state of the one-dimensional harmonic oscillator, we are able to define the ground state  $|A_0\rangle$  and two complex conjugate eigenstates  $|E_a\rangle$  and  $|E_b\rangle$  of the degenerate level. They equal to:  $|A_0\rangle = \psi_0(x)\psi_0(y)$ ,  $|E_a\rangle = (\psi_0(x)\psi_1(y) + i\psi_1(x)\psi_0(y))/\sqrt{2}$ , and  $|E_b\rangle = (\psi_0(x)\psi_1(y) - i\psi_1(x)\psi_0(y))/\sqrt{2}$ . In this case, the square norm of the transition matrix element is equal to  $|X|^2 = \hbar/4m^*\omega$ . Using the energy difference of the ground and the first excited energy level  $\epsilon = \hbar\omega$  and the confinement length  $l = \sqrt{\hbar/m^*\omega}$ , an expression for the dipole moment is obtained [22]

$$\mathbf{d}_{\uparrow\downarrow}^{\text{iho}} = \frac{|g|\mu_B B m^* l^4}{2l_{\text{so}} \hbar^2} (v_x \mathbf{e}_x + v_y \mathbf{e}_y). \quad (26)$$

## B. Dipole moment for systems with $\mathbf{C}_{2v}$ or $\mathbf{C}_{1v}$ symmetry

As the next step, we discuss potentials with  $\mathbf{C}_{2v}$  symmetry. In this case, coordinates  $x$  and  $y$  transform according to the IRs  $B_1$  and  $A_1$ , respectively. Their symmetry behaviour imposes the following:  $x(y)$  couples the ground state  $|A_0\rangle$  with states transforming according to the IR  $B_1(A_1)$  (see the right panel of FIG. 2). Thus, the SOI induced corrections of the qubit states are

$$\begin{aligned} |\delta A_{0\pm}\rangle &= \frac{|g|\mu_B B}{2l_{\text{so}}} \sum_i \left( \frac{\langle B_1^i | x v_x | A_0 \rangle}{\epsilon_{B_1}^i} |B_1^i \mp\rangle \right. \\ &\quad \left. + \frac{\langle A_1^i | y v_y | A_0 \rangle}{\epsilon_{A_1}^i} |A_1^i \mp\rangle \right), \end{aligned} \quad (27)$$

where  $\epsilon_{B_1}^i (\epsilon_{A_1}^i)$  is the energy difference between the energy level transforming according to the IR  $B_1(A_1)$  and the ground state energy. We define transition matrix elements as

$$X^i = \langle B_1^i | x | A_0 \rangle, Y^i = \langle A_1^i | y | A_0 \rangle, \quad (28)$$

and obtain the formula for the dipole moment

$$\mathbf{d}_{\uparrow\downarrow}^{\mathbf{C}_{2v}} = \frac{|g|\mu_B B}{l_{\text{so}}} \sum_i \left( \frac{|X^i|^2}{\epsilon_{B_1}^i} v_x \mathbf{e}_x + \frac{|Y^i|^2}{\epsilon_{A_1}^i} v_y \mathbf{e}_y \right). \quad (29)$$

In this case, anisotropy of the dipole moment appears since it is not forbidden that  $\sum_i |X^i|^2 / \epsilon_{B_1}^i$  differs from  $\sum_i |Y^i|^2 / \epsilon_{A_1}^i$ .

The anisotropy of the dipole moment can be illuminated using the example of the anisotropic two-dimensional harmonic potential  $V^{\text{aho}}(x, y) = 1/2m^*(\omega_x^2 x^2 + \omega_y^2 y^2)$ , with different confinement lengths  $l_x = \sqrt{\hbar/m^*\omega_x}$  and  $l_y = \sqrt{\hbar/m^*\omega_y}$  along the  $x$  and  $y$  direction. We set  $l = l_x$  and  $l_y = kl$ , where  $k < 1$  is the measure of anisotropy. We assume two excited orbital states in the perturbative correction: one of the type  $A_1$  and one of the type  $B_1$ . In this case we define the ground state  $|A_0\rangle = \psi_0(x)\psi_0(y)$  and two excited orbital states  $|A_1\rangle = \psi_0(x)\psi_1(y)$  and  $|B_1\rangle = \psi_1(x)\psi_0(y)$ , where  $\psi_{0/1}(x/y)$  represent the ground/first excited state of the one-dimensional harmonic oscillator problem in the  $x/y$  direction. The obtained result

$$\mathbf{d}_{\uparrow\downarrow}^{\text{aho}} = \frac{|g|\mu_B B m^* l^4}{2l_{\text{so}}\hbar^2} (v_x \mathbf{e}_x + k^4 v_y \mathbf{e}_y) \quad (30)$$

is again consistent with [22].

In the case of the  $\mathbf{C}_{1v}$  symmetry, using a similar analysis as in the previous case, we obtain the expression for the dipole moment

$$\mathbf{d}_{\uparrow\downarrow}^{\mathbf{C}_{1v}} = \frac{|g|\mu_B B}{l_{\text{so}}} \sum_i \left( \frac{|X^i|^2}{\epsilon_{B_0}^i} v_x \mathbf{e}_x + \frac{|Y^i|^2}{\epsilon_{A_0}^i} v_y \mathbf{e}_y \right), \quad (31)$$

where  $X^i = \langle B_0^i | x | A_0 \rangle$ ,  $Y^i = \langle A_0^i | y | A_0 \rangle$ , while  $\epsilon_{A_0/B_0}^i$  is the energy difference between the non-degenerate energy level transforming according to the IR  $A_0/B_0$  and the ground state energy.

### C. Dipole moment for systems with $\mathbf{C}_n$ or $\mathbf{C}_\infty$ symmetry

In the case of the  $\mathbf{C}_n$  symmetry, all IRs  $A_m$  ( $m \in (-n/2, n/2]$ ) are one-dimensional and represent an element of symmetry  $C_n^s$  ( $s = 0, 1, \dots, n-1$ ) as  $e^{i2\pi ms/n}$ . Beside the geometric symmetry, the time-reversal symmetry  $\Theta$  should be included also [37]. Time-reversal  $\Theta$  changes the sign of the quantum number  $m$  labeling the IR vector  $|A_m\rangle$ , since it acts as a complex conjugation in the orbital space

$$\Theta |A_m\rangle = |A_{-m}\rangle. \quad (32)$$

Eigenproblem of the Hamiltonian  $H|A_m\rangle = \epsilon_m |A_m\rangle$ , when combined with the commutation relation  $[\Theta, H_0] = 0$ , gives us

$$H|A_{-m}\rangle = \epsilon_m |A_{-m}\rangle, \quad (33)$$

stating that, for  $n \geq 3$ , vectors  $|A_m\rangle$  and  $|A_{-m}\rangle$  are eigenstates of the degenerate level  $\epsilon_m$ . To this degenerate level corresponds the reducible representation  $A_m \oplus A_{-m}$  (except for  $m = n/2$ ). The representation  $A_m \oplus A_{-m}$  is

equivalent to the IR  $E_m$  of the  $\mathbf{C}_{nv}$  group (see Table I) if the generator  $\sigma_v$  is neglected. In other words, Eq. (22) for the dipole moment is valid also in this case, since it is obtained without assuming the presence of vertical mirror symmetry. In this case vectors  $|E_a^i\rangle$  and  $|E_b^i\rangle$  coincide with  $|A_1^i\rangle$  and  $|A_{-1}^i\rangle$ , respectively.

A further simplification of the Eq. (22) appears for systems whose symmetry element is  $\pi/2$  rotation. This happens if the relation  $n = 4r$  ( $r \in \mathbb{N}$ ) is satisfied. Since  $(X^i)^* Y^i + X^i (Y^i)^* = 0$  and  $|X^i|^2 = |Y^i|^2$  in this case, Eq. (25) is relevant. Using the same reasoning it can be concluded that Eq. (25) is valid in the  $\mathbf{C}_\infty$  case also.

Finally, the dipole moment components (in  $|g|\mu_B B/l_{\text{so}}$  units) for the  $\mathbf{C}_2$  symmetry are equal to

$$\begin{aligned} (\mathbf{d}_{\uparrow\downarrow}^{\mathbf{C}_2})_x &= \frac{1}{2} \sum_i \left( \frac{2|X^i|^2 v_x + (X^i (Y^i)^* + (X^i)^* Y^i) v_y}{\epsilon_{A_1}^i} \right), \\ (\mathbf{d}_{\uparrow\downarrow}^{\mathbf{C}_2})_y &= \frac{1}{2} \sum_i \left( \frac{2|Y^i|^2 v_y + (X^i (Y^i)^* + (X^i)^* Y^i) v_x}{\epsilon_{A_1}^i} \right), \end{aligned} \quad (34)$$

where  $X^i = \langle A_1^i | x | A_0 \rangle$ ,  $Y^i = \langle A_1^i | y | A_0 \rangle$ , while  $\epsilon_{A_1}^i$  is the energy difference between the level transforming according to the IR  $A_1$  and the ground state energy.

To conclude, anisotropy of the potential orientation with respect to the crystallographic frame is present in systems without the  $\pi/2$  group element ( $n \neq 4r$ ,  $r \in \mathbb{N}$ ); isotropic behaviour is present if a rotation for  $\pi/2$  is the group element, i.e. if  $n = 4r$  ( $r \in \mathbb{N}$ ) or  $n = \infty$ .

## V. APPLICATIONS: EQUILATERAL TRIANGLE, SQUARE, AND RECTANGULAR POTENTIAL

The results presented in the previous Section fully explain the dependence of the Rabi frequency and spin relaxation rate on the spin-orbit angle, magnetic field direction, and the relative orientation of the gating potential with respect to the crystallographic frame.

However, symmetry arguments itself can not provide us with a qualitative estimation of the spin relaxation rate, corresponding to the phonon allowed spin qubit lifetime. Since  $\Gamma_{\uparrow\downarrow}$  is known for the harmonic gating [22], we wish to compare the phonon induced spin relaxation rate of other confinement potentials with the known values. To this end, we analyze the spin qubit confined inside an equilateral triangle, square and rectangular gating potential (see FIG. 3)

$$V^{\text{tqd}} = \begin{cases} 0, & x \in [\frac{y\sqrt{3}-a}{3}, \frac{a-y\sqrt{3}}{3}], y \in [\frac{-a\sqrt{3}}{6}, \frac{a\sqrt{3}}{3}], \\ \infty, & \text{otherwise.} \end{cases} \quad (35)$$

$$V^{\text{rqd}} = \begin{cases} 0, & x \in [-\frac{a}{2}, \frac{a}{2}], y \in [-\frac{b}{2}, \frac{b}{2}], \\ \infty, & \text{otherwise.} \end{cases} \quad (36)$$

In the first case, Eq. (35), the potential has  $\mathbf{C}_{3v}$  symmetry and the corresponding eigenvectors of the spin-independent Hamiltonian  $H_0$  transform according to the

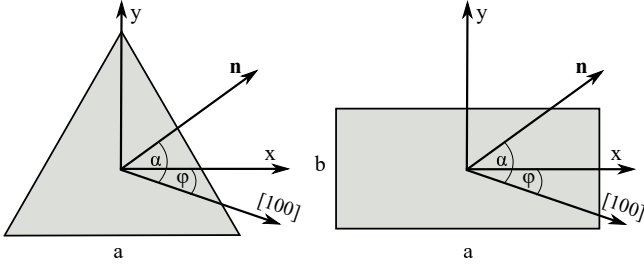


FIG. 3. Equilateral triangle (left panel) and rectangular (right panel) gating potential. In both cases, potential is zero inside the area of the polygon, otherwise it is  $\infty$ .

one-dimensional IRs  $A_0$ ,  $B_0$  and two-dimensional  $E_1$  IR of the  $C_{3v}$  group. The set of eigenenergies  $\epsilon_{p,q}^{\text{tqd}}$  and eigenvectors  $\psi_{p,q}^{A_0}$ ,  $\psi_{p,q}^{B_0}$  and  $\psi_{p,q}^{E_1\pm}$  [38] are dependent on two parameters  $p$  and  $q$  that have different set of allowed values for each IR. Their concrete form is given in Appendix A.

In the second case, Eq. (36), symmetry of the potential is dependent on the ratio  $k = b/a \in (0, 1]$ : if  $k = 1$ , symmetry of the problem is  $C_{4v}$ ; otherwise,  $C_{2v}$  is the symmetry of spin-independent Hamiltonian  $H_0$ . In both situations, eigenenergies and eigenvalues can be found by using the separation of variables. The set of eigenenergies  $\epsilon_{p,q}^{\text{rqd}}$  and eigenvectors  $\psi_{p,q}^{\text{rqd}}$  in this case is

$$\epsilon_{p,q}^{\text{rqd}} = \frac{\hbar^2 \pi^2}{2m^* a^2} (p^2 + \frac{q^2}{k^2}), \quad (37)$$

$$\psi_{p,q}^{\text{rqd}} = \frac{2}{a\sqrt{k}} \sin\left[\frac{p\pi}{a}(x + \frac{a}{2})\right] \sin\left[\frac{q\pi}{ak}(y + \frac{ka}{2})\right], \quad (38)$$

defined using the two independent parameters  $p \geq 1$  and  $q \geq 1$  that take integer values. However, these solutions do not have any definite symmetry [39]. Therefore, they need to be symmetrized to apply the general results from Section IV. Symmetry adapted eigenfunctions can be found in Appendix B.

After calculating the transition dipole matrix element and the excitation energies for two excited states in the perturbative correction [40], we obtain the desired results

$$\mathbf{d}_{\uparrow\downarrow}^{\text{tqd}} = \frac{3^{24}}{2^{26} 3^{52} \pi^8} \frac{|g| \mu_B B m^* a^4}{l_{\text{so}} \hbar^2} (v_x \mathbf{e}_x + v_y \mathbf{e}_y), \quad (39)$$

$$\mathbf{d}_{\uparrow\downarrow}^{\text{rqd}} = \frac{2^9}{3^5 \pi^6} \frac{|g| \mu_B B m^* a^4}{l_{\text{so}} \hbar^2} (v_x \mathbf{e}_x + k^4 v_y \mathbf{e}_y), \quad (40)$$

where the first result corresponds to the equilateral triangle potential, while the second one is valid for both the square,  $k = 1$ , and rectangular,  $k \neq 1$ , potential. Dipole moment constants  $3^{24}/2^{26} 3^{52} \pi^8 \approx 3.6 \times 10^{-4}$  and  $2^9/3^5 \pi^6 \approx 2.2 \times 10^{-3}$  from Eqs. (39) and (40) suggest much weaker dipole moment, when compared to the harmonic gating of the same confinement length (see Eqs. (26) and (30)).

Using the relation  $\Gamma_{\uparrow\downarrow} \approx |\mathbf{d}_{\uparrow\downarrow}|^2$ , we conclude that square/rectangular confined QD has four orders of magnitude weaker relaxation rate than the harmonic potential; in the equilateral triangle case almost six orders of

magnitude decrease is observed. Thus, our result indicates a significant influence of the gating potential on the spin qubit lifetime and a beneficial role of the equilateral triangle confinement.

## VI. CONCLUSIONS

We have investigated the influence of the gating potential symmetry on the Rabi frequency and phonon induced spin relaxation rate in a single electron GaAs quantum dot. Our results suggest that, independently of the symmetry of the gating potential, both the Rabi frequency and spin relaxation rate are dependent on the orientation of the magnetic field and the spin-orbit angle. Additionally, in systems with  $C_{1v}$ ,  $C_{2v}$ , and  $C_n$  ( $n \neq 4r$ ) symmetry, orientation of the quantum dot potential with respect to the crystallographic reference frame is another degree of freedom that can be used to tune the desired properties of the system. The validity of the approach is confirmed on the known results for the isotropic and anisotropic harmonic potential. Additionally, we have compared the spin qubit lifetime in the case of a rectangular, square and equilateral triangle gating with the harmonic confinement. Our results indicate the enhanced lifetime of the spin qubit, reaching almost six orders of magnitude increase in the case of the equilateral triangle gating.

## ACKNOWLEDGMENTS

We thank Nenad Vukmirović for fruitful discussion. This research is funded by the Serbian Ministry of Science (Project ON171035).

### Appendix A: Particle in an equilateral triangle potential: eigenenergies and eigenvectors

Here we summarize the results from [38] regarding the Schrödinger equation solution of the particle in an equilateral triangle potential, having the  $C_{3v}$  symmetry. Due to the symmetry, eigenvectors transform according to the one-dimensional  $A_0$ ,  $B_0$  IRs and two-dimensional  $E_1$  IR. The concrete form of eigenenergies and eigenstates

$$\epsilon_{p,q}^{\text{tqd}} = \frac{8\hbar^2 \pi^2}{3m^* a^2} (p^2 + pq + q^2), \quad (A1)$$

$$\begin{aligned} \psi_{p,q}^{A_0}(x, y) = & \cos\left[\frac{2\pi q}{a}x\right] \sin\left[\frac{2\pi(2p+q)}{a\sqrt{3}}y\right] \\ & - \cos\left[\frac{2\pi p}{a}x\right] \sin\left[\frac{2\pi(p+2q)}{a\sqrt{3}}y\right] \\ & - \cos\left[\frac{2\pi(p+q)}{a}x\right] \sin\left[\frac{2\pi(p-q)}{a\sqrt{3}}y\right], \\ & q = 0, 1, 2, \dots, \quad p = q + 1, q + 2, \dots \end{aligned} \quad (A2)$$

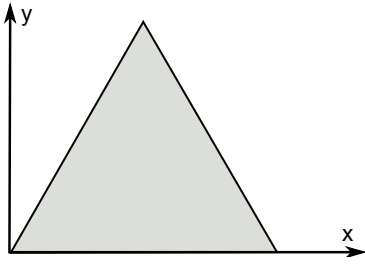


FIG. 4. Equilateral triangle potential with point group symmetry  $\mathbf{C}_{3v}$ . Inside the equilateral triangle potential is 0, otherwise it is  $\infty$ .

$$\begin{aligned} \psi_{p,q}^{B_0}(x,y) = & \sin\left[\frac{2\pi q}{a}x\right] \sin\left[\frac{2\pi(2p+q)}{a\sqrt{3}}y\right] \\ & - \sin\left[\frac{2\pi p}{a}x\right] \sin\left[\frac{2\pi(p+2q)}{a\sqrt{3}}y\right] \\ & + \sin\left[\frac{2\pi(p+q)}{a}x\right] \sin\left[\frac{2\pi(p-q)}{a\sqrt{3}}y\right], \\ q = 1, 2, 3, \dots, \quad p = q+1, q+2, \dots \end{aligned} \quad (\text{A3})$$

$$\begin{aligned} \psi_{p,q}^{E_{1\pm}}(x,y) = & \psi_{p,q}^{B_0}(x,y) \pm i\psi_{p,q}^{A_0}(x,y), \\ q = \frac{1}{3}, \frac{2}{3}, \frac{4}{3}, \frac{5}{3}, \dots, \quad p = q+1, q+2, \dots \end{aligned} \quad (\text{A4})$$

is dependent on two parameters  $p$  and  $q$  that have different allowed values for each IR. Note that the coordinate frame used to derive the previous equations (see FIG. 4) differs the frame used in our work (see the left panel of FIG. 3). To adapt the eigenfunction from Eqs. (A2-A4) to our case, suitable change of coordinates  $x \rightarrow x + a/2$  and  $y \rightarrow y + a\sqrt{3}/6$  should be made.

## Appendix B: Particle in a square and rectangular potential: eigenvectors

A square potential has the  $\mathbf{C}_{4v}$  symmetry with the corresponding IRs  $A_0/B_0$ ,  $A_2/B_2$  and  $E_1$ . Eigenvectors that transform according to the given IRs and the set of allowed quantum numbers are

$$\begin{aligned} \psi_{p,q}^{A_0}(x,y) = & \cos\left[\frac{p\pi}{a}x\right] \cos\left[\frac{q\pi}{a}y\right] + \cos\left[\frac{q\pi}{a}x\right] \cos\left[\frac{p\pi}{a}y\right] \\ q = 1, 3, 5, \dots, \quad p = q, q+2, q+4, \dots \end{aligned} \quad (\text{B1})$$

$$\begin{aligned} \psi_{p,q}^{B_0}(x,y) = & \sin\left[\frac{p\pi}{a}x\right] \sin\left[\frac{q\pi}{a}y\right] - \sin\left[\frac{q\pi}{a}x\right] \sin\left[\frac{p\pi}{a}y\right] \\ q = 2, 4, 6, \dots, \quad p = q+2, q+4, \dots \end{aligned} \quad (\text{B2})$$

$$\begin{aligned} \psi_{p,q}^{A_2}(x,y) = & \cos\left[\frac{p\pi}{a}x\right] \cos\left[\frac{q\pi}{a}y\right] - \cos\left[\frac{q\pi}{a}x\right] \cos\left[\frac{p\pi}{a}y\right] \\ q = 1, 3, 5, \dots, \quad p = q+2, q+4, \dots \end{aligned} \quad (\text{B3})$$

$$\begin{aligned} \psi_{p,q}^{B_2}(x,y) = & \sin\left[\frac{p\pi}{a}x\right] \sin\left[\frac{q\pi}{a}y\right] + \sin\left[\frac{q\pi}{a}x\right] \sin\left[\frac{p\pi}{a}y\right] \\ q = 2, 4, 6, \dots, \quad p = q, q+2, q+4, \dots \end{aligned} \quad (\text{B4})$$

$$\begin{aligned} \psi_{p,q}^{E_{1\pm}}(x,y) = & \cos\left[\frac{p\pi}{a}x\right] \sin\left[\frac{q\pi}{a}y\right] \pm i \sin\left[\frac{q\pi}{a}x\right] \cos\left[\frac{p\pi}{a}y\right] \\ p = 1, 3, 5, \dots, \quad q = p+1, p+3, \dots \end{aligned} \quad (\text{B5})$$

In the case of the rectangular potential  $\mathbf{C}_{2v}$  symmetry is relevant. Eigenfunctions transforming according to the IRs  $A_0/B_0$  and  $A_1/B_1$  and the corresponding set of quantum numbers are

$$\begin{aligned} \psi_{p,q}^{A_0}(x,y) = & \cos\left[\frac{p\pi}{a}x\right] \cos\left[\frac{q\pi}{ka}y\right] \\ q = 1, 3, 5, \dots, \quad p = q, q+2, q+4, \dots \end{aligned} \quad (\text{B6})$$

$$\begin{aligned} \psi_{p,q}^{B_0}(x,y) = & \sin\left[\frac{p\pi}{a}x\right] \sin\left[\frac{q\pi}{ka}y\right] \\ q = 2, 4, 6, \dots, \quad p = q, q+2, q+4, \dots \end{aligned} \quad (\text{B7})$$

$$\begin{aligned} \psi_{p,q}^{A_1}(x,y) = & \cos\left[\frac{p\pi}{a}x\right] \sin\left[\frac{q\pi}{ka}y\right] \\ p = 1, 3, 5, \dots, \quad q = p+1, p+3, p+5, \dots \end{aligned} \quad (\text{B8})$$

$$\begin{aligned} \psi_{p,q}^{B_1}(x,y) = & \sin\left[\frac{p\pi}{a}x\right] \cos\left[\frac{q\pi}{ka}y\right] \\ q = 1, 3, 5, \dots, \quad p = q+1, q+3, q+5, \dots \end{aligned} \quad (\text{B9})$$

In both cases, eigenenergies are given in Eq. (37) ( $k = 1$  in the  $\mathbf{C}_{4v}$  case,  $k \neq 1$  for the  $\mathbf{C}_{2v}$  symmetry).

- 
- [1] M. A. Nielsen and I. L. Chuang, *Quantum Computation and Quantum Information*, Cambridge University Press, (2010).
  - [2] C. H. Bennett and D. P. DiVincenzo, *Nature* **404**, 247-255 (2000).
  - [3] D. Loss and D. P. DiVincenzo, *Phys. Rev. A* **57**, 120 (1998).

- [4] T. P. Orlando, J. E. Mooij, L. Tian, C. H. van der Wal, L. S. Levitov, S. Lloyd, and J. J. Mazo, *Phys. Rev. B* **60**, 15398 (1999).
- [5] Y. Nakamura, Yu. A. Pashkin, and J. S. Tsai, *Nature* **398**, 786-788 (1999).
- [6] M. Yamamoto, S. Takada, C. Bäuerle, K. Watanabe, A. D. Wieck, and S. Tarucha, *Nat. Nanotechnol.* **7**, 247-251 (2012).



- [7] E. I. Rashba, *Sov. Phys. Solid State* **2**, 1109 (1960).
- [8] V. N. Golovach, M. Borhani, and D. Loss, *Phys. Rev. B* **74**, 165319 (2006).
- [9] D. V. Bulaev and D. Loss, *Phys. Rev. Lett.* **98**, 097202 (2007).
- [10] K. C. Nowack, F. H. L. Koppens, Yu. V. Nazarov, and L. M. K. Vandersypen, *Science* **318**, 1430-1433 (2007).
- [11] E. I. Rashba, *Phys. Rev. B* **78**, 195302 (2008).
- [12] R. Brunner, Y.-S. Shin, T. Obata, M. Pioro-Ladrière, T. Kubo, K. Yoshida, T. Taniyama, Y. Tokura, and S. Tarucha, *Phys. Rev. Lett.* **107**, 146801 (2011).
- [13] E. Kawakami, P. Scarlino, D. R. Ward, F. R. Braakman, D. E. Savage, M. G. Lagally, Mark Friesen, S. N. Coppersmith, M. A. Eriksson, and L. M. K. Vandersypen, *Nat. Nanotechnol.* **9**, 666-670 (2014).
- [14] K. Takeda, J. Yoneda, T. Otsuka, T. Nakajima, M. R. Delbecq, G. Allison, Y. Hoshi, N. Usami, K. M. Itoh, S. Oda, T. Koderia, and S. Tarucha, *npj Quantum Inf.* **4**, 54 (2018).
- [15] D. V. Khomitsky, E. A. Lavrakhina, and E. Ya. Sherman, *Phys. Rev. B* **99**, 014308 (2019).
- [16] S. Studenikin, M. Korkusinski, M. Takahashi, J. Ducautel, A. Padawer-Blatt, A. Bogan, D. Guy Austing, L. Gaudreau, P. Zawadzki, A. Sachrajda, Y. Hirayama, L. Tracy, J. Reno, and T. Hargett, *Commun. Phys.* **2**, 159 (2019).
- [17] A. V. Khaetskii and Y. V. Nazarov, *Phys. Rev. B* **61**, 12639 (2000); A. V. Khaetskii and Y. V. Nazarov, *Phys. Rev. B* **64**, 125316 (2001).
- [18] P. Stano and J. Fabian, *Phys. Rev. B* **72**, 155410 (2005); F. Baruffa, P. Stano, and J. Fabian, *Phys. Rev. Lett.* **104**, 126401 (2010).
- [19] V. N. Stavrou, *J. Phys.: Condens. Matter* **29**, 485301 (2017); V. N. Stavrou, *J. Phys.: Condens. Matter* **30**, 455301 (2018).
- [20] Z.-H. Liu, R. Li, X. Hu and J. Q. You, *Sci. Rep.* **8**, 2302 (2018).
- [21] J. I. Climente, A. Bertoni, G. Goldoni, M. Rontani, and E. Molinari, *Phys. Rev. B* **75**, 081303(R) (2007).
- [22] O. Malkoc, P. Stano, and D. Loss, *Phys. Rev. B* **93**, 235413 (2016).
- [23] D. Chaney and P. A. Maksym, *Phys. Rev. B* **75**, 035323 (2007).
- [24] V. I. Fal'ko, B. L. Altshuler, and O. Tsypliyatyev, *Phys. Rev. Lett.* **95**, 076603 (2005).
- [25] P. Scarlino, E. Kawakami, P. Stano, M. Shafiei, C. Reichl, W. Wegscheider, and L. M. K. Vandersypen, *Phys. Rev. Lett.* **113**, 256802 (2014).
- [26] M. Raith, P. Stano, and J. Fabian, *Phys. Rev. B* **83**, 195318 (2011).
- [27] G. Dresselhaus, *Phys. Rev.* **100**, 580 (1955).
- [28] E. I. Rashba, *Fiz. Tv. Tela (Leningrad)* **2**, 1224 (1960); *Sov. Phys. Solid State* **2**, 1109 (1960).
- [29] M. Raith, T. Pangerl, P. Stano, and J. Fabian, *Phys. Status Solidi b* **251**, 1924 (2014).
- [30] R. de Sousa and S. Das Sarma, *Phys. Rev. B* **68**, 155330 (2003).
- [31] Note that both the wave vector  $\mathbf{q}$  and the electron coordinate  $\mathbf{r}_e$  are written in the crystallographic reference frame.
- [32] J. I. Climente, A. Bertoni, G. Goldoni, and E. Molinari, *Phys. Rev. B* **74**, 035313 (2006).
- [33] J. L. Cheng, M. W. Wu, and C. Lü, *Phys. Rev. B* **69**, 115318 (2004).
- [34] L. C. Camenzind, L. Yu, P. Stano, J. D. Zimmerman, A. C. Gossard, D. Loss, and D. M. Zumbühl, *Nat. Commun.* **9**, 3454 (2018).
- [35] E. Lijnen, L. F. Chibotaru, and A. Ceulemans, *Phys. Rev. E* **77**, 016702 (2008).
- [36] L. Jansen and M. Boon, *Theory of Finite Groups: Applications in Physics*, North Holland, Amsterdam, (1967); M. Damnjanović, *O simetriji u kvantnoj nerelativističkoj fizici*, Fizički fakultet, Beograd (2000). <http://www.ff.ac.rs/Katedre/QMF/SiteQMF/pdf/sknf2e.pdf>
- [37] In the case of  $C_{nv}/C_{\infty v}$  groups, time-reversal  $\Theta$  is the symmetry of the system. However, it can be checked that  $\Theta$  can be safely neglected. Time-reversal in the case of vectors from one-dimensional IRs has a trivial action. In the case of the two-dimensional IRs  $E_m$  time-reversal transforms one vector of the IR into the other; in other words, it has the same behaviour as the vertical mirror plane symmetry  $\sigma_v$  and can be ignored.
- [38] W.-K. Li and S. M. Blinder, *J. Math. Phys.* **26**, 2784 (1985).
- [39] L. F. Chibotaru, A. Ceulemans, M. Morelle, G. Teniers, C. Carballeira, and V. V. Moshchalkov, *J. Math. Phys.* **46**, 095108 (2005).
- [40] We have explicitly checked that other states appearing in the perturbative expansion can be safely ignored.